

## Ceramic Foams: Synthesis, Characterisation and Exploration in the Adsorption of Ni<sup>2+</sup> and Cr<sup>3+</sup> from Aqueous Solutions

RAFAEL A. FONSECA<sup>a</sup>, LILIANA GIRALDO<sup>b</sup> and  
JUAN CARLOS MORENO-PIRAJÁN<sup>a\*</sup>

<sup>a</sup>Facultad de Ciencias, Departamento de Química, Grupo de Investigación de Sólidos Porosos y Calorimetría, Universidad de Los Andes, Bogotá, Colombia

<sup>b</sup>Facultad de Ciencias, Departamento de Química, Universidad Nacional de Colombia  
*jumoreno@uniandes.edu.co*

Received 6 January 2013 / Accepted 14 February 2013

**Abstract:** Ceramic foams are synthesised by three technical replicates. The foams are characterised by SEM techniques, FTIR, nitrogen adsorption isotherms at 77 K and the Instron test. Subsequently, foams are used for the adsorption of Ni<sup>2+</sup> and Cr<sup>3+</sup> from aqueous solution. The results show that the foam EC-1 has the highest adsorption capacity for both ions at the working pH. The adsorption of the studied ions was adjusted by the Freundlich model.

**Keywords:** Foams ceramics, Adsorption, Isotherms, Freundlich model, Ions metallic

### Introduction

Plastic foams were the first to be synthesised between 1950 and the mid-1970s; Yajima *et al.*<sup>1</sup> reported the synthesis of ceramic foams. The first method developed for ceramic foams is called the polymeric foam method; today, there are two other methods reported in the literature for obtaining ceramic foams, which are the sol-gel process or gelation and the synthesis of polymers through pre-ceramics.

Porous ceramics are of great interest due to their numerous potential applications in the catalysis, adsorption, separation and filtration of molten metals or hot gases and the refractory insulation of furnaces, as well as other trends involved in engineering<sup>2,3</sup>. The three main processing routes for the fabrication of macroporous ceramics are the replica technique, the sacrificial template method and the direct-foaming technique. The processing route ultimately determines the microstructure of the final macroporous ceramic<sup>4,5</sup>. Therefore, the selection of a given processing method depends strongly on the microstructure needed for the end application, as well as on the inherent features of the process, such as cost, simplicity and versatility<sup>5</sup>.

With industrial development, heavy pollution in the air and in water bodies has been caused. Therefore, in the last few decades, some of the most interesting work in the area of solid materials has been developed to remove these pollutants with high efficiency and low cost.

It is known that compounds in the liquid phase can be treated by physicochemical processes and chemical, physical and biological factors. Of all these processes, the most widely used is physicochemical adsorption using adsorbents such as silica, zeolites and activated carbon, *etc.* Demand has increased in recent years; in the U.S. there has been an average annual increase of 6.6% for use in treating water<sup>6</sup>.

The adsorption capacity is the most important property of the adsorbents; the value of this parameter determines the amount of water that can be treated per unit mass or volume. The adsorption capacity is related to the surface area, porosity and surface chemistry of the porous solid<sup>7</sup>.

The process of production of ceramic foams from pre-ceramic polymers is currently being studied because the foams obtained by this method are capable of controlling cell size and rigid foams are obtained which are widely used in a large number of catalytic processes. The scope of this work involves the synthesis of ceramic foams using the replica method, varying the percentages of the components of the foam and analysing the effects on the adsorption capacity of nickel and chromium.

## Experimental

In this technique, a suspension is impregnated with ceramic materials, which generate pores. They can be used as synthetic and natural materials, polymeric foam, wood, coral, marine skeletons, *etc.*

Polymeric foam is used to synthesise ceramic foams, because it is the more known method and that works better. The process is based on a ceramic mixture prepared previously (Table 1) in which polymeric foam is inserted; in this work, this was polyurethane (PU). The foam is subsequently subjected to a drying process and finally sintered at 1523 K, producing ceramic foam with a negative structure of the polymer foam used. Mixtures used for obtaining ceramic foams are shown in Table 1, with compositions containing varied feldspar and quartz levels, which are the two components responsible for providing the structure in the sintering process.

**Table 1.** Percentage ratios ceramic mixtures and nomenclature

Ceramic Foam	% Clay	% Quartz	% Kaolin	% Feldspar
EC-1	10	30	40	20
EC-2	10	20	40	30
EC-3	10	10	40	40

### *Adsorbates*

For the study of the behaviour of the adsorption capacity of the ceramics synthesised in this work, the ions  $\text{Cr}^{3+}$  and  $\text{Ni}^{2+}$  were used as adsorbates. Solutions were prepared from their corresponding salts, such as nitric, using analytical grade reagents for solutions with concentrations within the range of 20 to 500 ppm. All solutions were prepared by dilution with deionised water and their concentrations were determined using the atomic absorption technique; the results were compared with a previously prepared calibration curve.

### *Textural characterisation; N<sub>2</sub> adsorption isotherms at 77 K*

The textural characterisation of ceramic foams was performed by physical adsorption of  $\text{N}_2$  at 77 K. To perform these analyses, the samples were previously degassed at 423 K for 24 h. The apparent surface area was calculated using the BET equation, the micropore volume  $V_0$ .

(N<sub>2</sub>) was obtained by applying the Dubinin-Radushkevich equation to the data of the adsorption of nitrogen (liquid N<sub>2</sub> Density = 0808 g/cm<sup>3</sup>). The total pore volume V<sub>t</sub> was calculated from the volume adsorbed at relative pressures of 0.99, and the mesopore volume was calculated by the difference<sup>8</sup>. For these determinations, automatic sortometer of Quantachrome IQ2 Instruments (Boynton Beach, Miami, FL, USA) was employed. Carbonaceous samples EC-1, EC-2 and EC-3, about 0.100 g, were analysed by this method.

#### *Characterisation by the technique of X-ray diffraction*

The x-ray diffraction of the ceramic foam prepared materials was performed using an x-ray diffractometer with CuK $\alpha$  radiation at 40 kV and 14 mA. Ceramic foams were macerated to a fine powder before performing the measurement with this technique. The powder was placed in a bracket for measuring the X-ray spectrum, the data are taken from 5° <2 $\theta$  <70° at a rate of 5° (2 $\theta$ ) per minute.

#### *Infrared spectroscopy (FT-IR)*

The samples were analysed by infrared spectroscopy; 0.1 g of each ceramic foam was crushed and mixed with potassium bromide (to remove the dispersal effects of large crystals). This powder mixture was compressed in a die press to form a mechanically translucent tablet through which the light beam of the spectrometer can pass. The results were read on a Thermo-Nicolet 6700 FT-IR.

#### *Scanning electron microscopy (SEM)*

The SEM consists of an optical column and an electronic console. The former has a chamber that is under high vacuum (approximately 2x10<sup>-6</sup> torr), where the sample to be analysed is placed. The image is formed by an electron beam directed towards the sample; this beam is generated from an electron gun, which is a tungsten filament cathode heated by a thermionic emission system to a temperature exceeding 2700 K. The filament emits electrons, which produce high negative potential in abundance relative to the anode; they are rapidly accelerated towards the same column via the electronics. The electron beam passes through electromagnetic lenses of two or three capacitors whose function is to reduce the beam diameter. Any radiation from the sample can be used to provide a signal and each one of which is the result of some interaction between the incident electrons and the specimen, providing different information<sup>8,9</sup>.

A microscope is an optical system that magnifies small objects for examination under natural light or light emitted from an artificial source; in electron microscopy, an electron beam is used instead of light to form the image. An SEM has a magnification range of 10 to 180,000 X and with x-ray detectors, allows very small minerals to be identified and examines the shape and distribution of these<sup>9</sup>.

The scanning electron microscope allows the morphology and porosity of the materials to be observed directly. In this technique, a beam of electrons in the vacuum causes the excitation of secondary electrons in the sample, which generate signals that are picked up as an image. The details of this depend on the magnification taken used.

#### *Determination of adsorption capacity of contaminant metal ions Cr<sup>3+</sup> and Ni<sup>2+</sup> from aqueous solutions*

The data of adsorption isotherms was obtained by mixing 0.1 g of each solid with a volume of 25 mL of metal solutions of known initial concentrations ranging from 20 to 500 mgL<sup>-1</sup>, the pH was adjusted to 5.0 at 298 K for 96 hours; then, the concentration of ions was calculated under the same conditions used for the calibration curve.

Adsorption was performed separately for each ion in the obtained porous solid samples; the pH of each ion was adjusted with  $\text{HNO}_3/\text{NaOH}$  diluted by dropwise addition<sup>10</sup>. Solutions containing 20, 50, 100, 150, 200 and 500 ppm were prepared in 25 mL volumes. To evaluate the adsorption capacity, measurements were performed regarding the decrease of concentration after 96 hours.

This experiment was carried out using an assembly that was particularly designed to determine the changes in concentrations. This assembly will be called here the adsorber lot (or batch type), which is shown in Figure 1. The adsorber consists of a conical flask of 50 or 100 mL which is placed in the solution of the solute or adsorbate with the porous solid. The latter is placed in a bag made of nylon mesh, in order to ensure that there is no friction between the particles themselves and the container wall and thus preventing the formation of fine powders of carbon or ceramics that may interfere in the analysis of ions in an aqueous solution.

The flask adsorber was partially introduced in a constant temperature bath to maintain a constant temperature of the solution. The constant temperature bath consisted of an acrylic container and a water recirculator. The solution was kept under constant stirring using a magnetic stirrer; the teflon casing was actuated by a magnetic plate placed under the constant temperature bath.

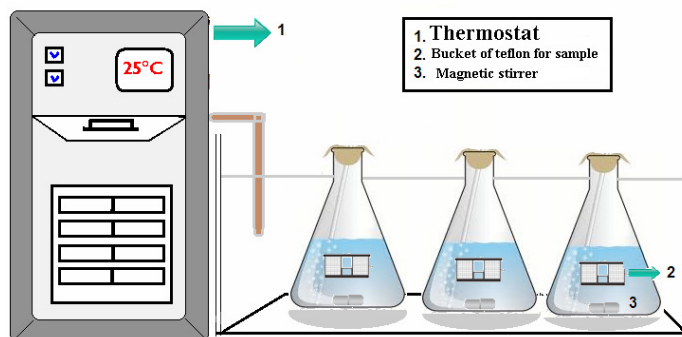


**Figure 1.** Batch adsorber for the study of adsorption at the solid-liquid

## Results and Discussion

### *Infrared spectra results of the ceramic foams*

Figure 2 shows the infrared spectra taken corresponding to each of the ceramics synthesised in this work in the range of  $500\text{-}4000\text{ cm}^{-1}$ . The bands that appear in the respective IR correspond to the vibration characteristics of each mixture component: clays, feldspar, quartz and kaolin. EC-1 for the IR bands-associated Kaolin vibrations correspond to the links of the structure, the Si-O tetrahedra Si, Al-O and Al-OH of aluminium octahedra and Si-O-Al  $\text{SiO}_4\text{-AlO}_4$  unions. In the case of contamination by quartz, this may occur simultaneously with other bands characteristic of this material. In general, the most intense Kaolin characteristic bands should appear as follows:  $3694, 3621, 1100, 1032, 1008, 913, 694, 539, 471$  and  $431\text{ cm}^{-1}$ , although variations<sup>11</sup> may occur, especially at wavelengths between  $3695$  and  $3620\text{ cm}^{-1}$  due to the low crystallinity of Kaolin<sup>12</sup>.

Regarding the samples EC-2 and EC-3, it was observed that the characteristic bands located at Kaolin  $3694, 3620$  and  $911\text{ cm}^{-1}$  weakened, mainly because it altered the composition of the mixture, causing this kind of behaviour in this spectrum.

In general, the IR study samples were found to be EC-1, EC-2 and EC-3; the characteristic bands are the main components of Kaolin and Feldspar mixtures located at 3695, 3652 and 3260  $\text{cm}^{-1}$ , corresponding to vibrations of the OH bonds of both Al-OH groups and water. Also, the bands at 1032, 1000 and 911  $\text{cm}^{-1}$  should be appreciated for Si-O vibration Al-O and Al-OH groups, as those are attributable to Si-O-Al located in 750, 695 and 536  $\text{cm}^{-1}$ . These results agree with those reported by XRD.

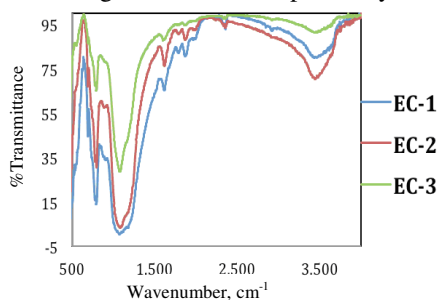


**Figure 2.** Infrared spectrum corresponding to the ceramic foams synthesised

*Study by scanning electron microscopy for each ceramic foam*

The samples were also characterised by the technique of microscopy (SEM). Figure 3 presents some images corresponding to the ceramic foams synthesised in this work; the general characteristics of each material can be seen in these micrographs. The analysis corroborated the presence of pores, the development of which is strongly dependent on the composition of each mixture.

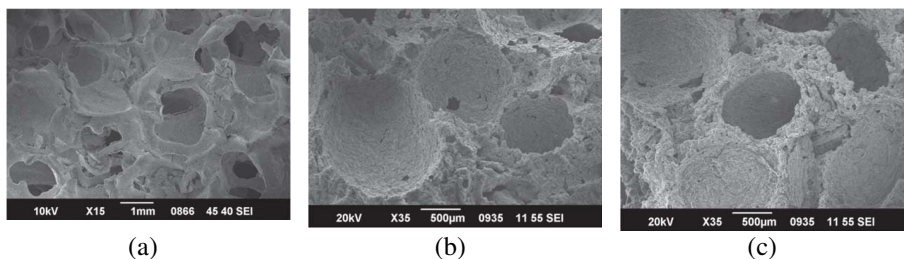


**Figure 3.** SEM of synthesised ceramic foams: (a) EC-1 (b) EC-2 (c) EC-3

By observing in detail a change in the micrographs, the porosity is observed, which is associated with the change in the contents of Kaolin and fundamentally feldspar.

*XRD study of the ceramic foams*

Figure 4 shows each of the peaks corresponding to mixtures of the ceramic foams prepared: Figure 5(a) corresponds to the EC-1, Figure 5 (b) corresponds to the sample EC-2 and Figure 5(c) corresponds to the EC-3 foam. In each of the DRX, peaks are presented at angles well defined as those that occurring between 27°-30°, which correspond to kaolin; other peaks that can be associated with the presence of this material are those found in the positions 21° and 40° where intensities change is due to the composition of each material<sup>12</sup>. XRD also shows the presence of quartz at 40° and 50°, whose intensities again changed according to the composition in each mixture. The presence of feldspar reinforced and enhanced the signals at angles of 21° and 40°, which demonstrates the presence and incorporation of each of the materials that compose each one of the ceramic foams.

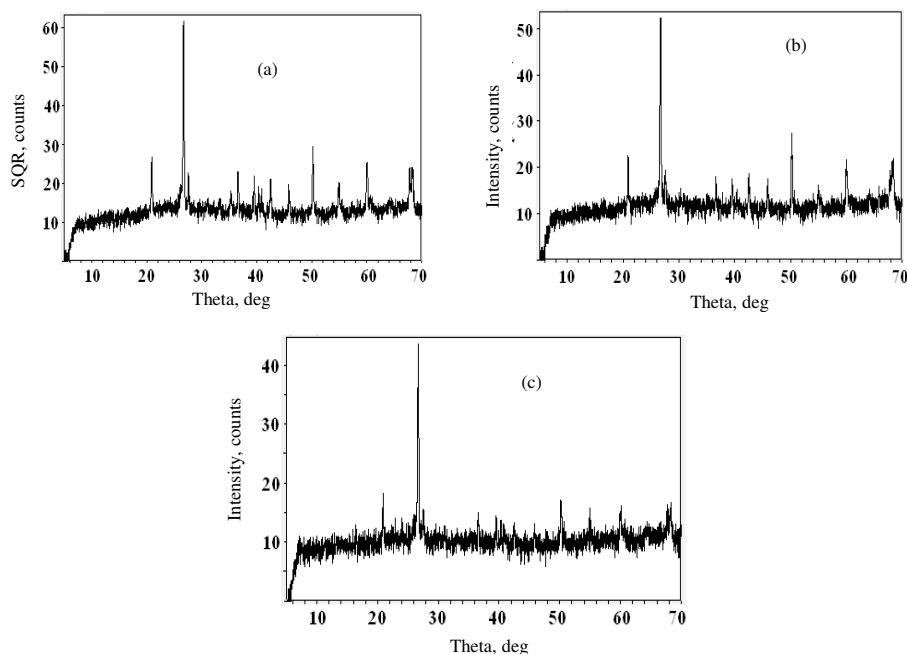
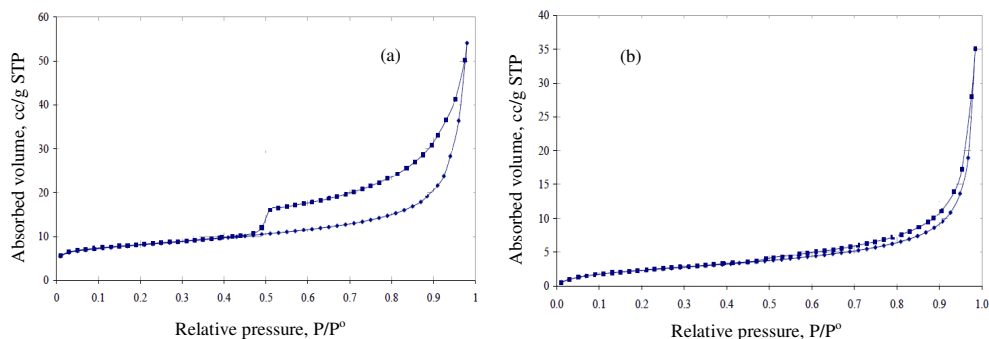


**Figure 4.** X-ray diffraction pattern of each of the ceramic foams prepared: a) EC-1 (b) EC-2 and (c) EC-3

#### *Textural analysis of ceramic foams*

Textural analysis was performed on samples from the adsorption-desorption isotherm of nitrogen at 77 K. The initial part of the isotherms (at low relative pressures) corresponds to the formation of the monolayer, and the remaining multilayer adsorption. According to Figure 5, the marked rise of the isotherms at low pressures indicates few or no micropores. The shape of the curves at higher pressures indicates the presence of mesopores.

As established by the theory of BET specific area, at relative pressures less than 0.30, the calculation  $(1/V) \{P^0 / (P^0 - 1)\} - 1$  vs.  $P / P^0$  is plotted; we obtained the molar volume of the monolayer  $V_m$ . Other variables are as follows:  $V$  is the volume adsorbed at a pressure  $P$ , saturation pressure is  $P^0$  and  $m$  is the mass in grams adsorbent. Table 3 shows the values of the BET specific areas of the different samples.



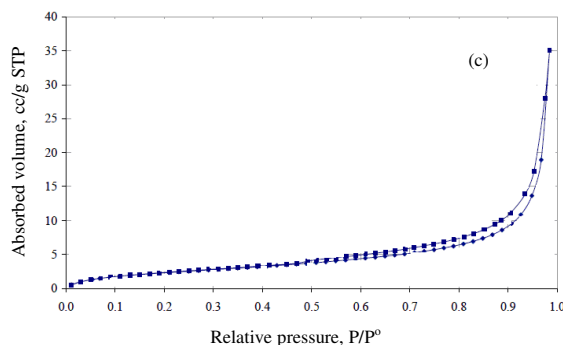


**Figure 5.** Adsorption-desorption isotherms of  $N_2$  at 77 K for the ceramic foams: (a) EC-1, (b) EC-2) and (c) EC-3

Comparing the isotherms obtained for the different samples (Figure 5) shows the hysteresis loops corresponding to  $H_3$  type according to the IUPAC causing the type of porosity. In this case it is observed that the feldspar component is the one that is modified to a greater degree of porosity changes in the foams, as shown in Figures 5(a), (b) and (c).

Table 2 presents the main textural parameters of ceramic foams; it is worth noting that the greatest development was the BET area EC-1, which is in good agreement with previous results obtained with SEM.

**Table 2.** Textural parameters of ceramic foams determined by the  $N_2$  adsorption isotherms at 77 K

Ceramic Foam	$S_{BET}$ , $m^2/g$	$V_{Pore}$ , $cm^3/g$	Average pore size, nm
EC-1	35	0.97	17.8
EC-2	26	0.034	12.3
EC-3	14	0.023	9.6

### Study compressive strength

It is important to know whether a material such as ceramic foam is resistant or not, because in this work was used as adsorbent of pollutants, so it is important to measure its strength. The compressive strength is determined by calculating the compression elastic modulus of the ceramic material through the treatment of the data obtained after performing the experimental method according to ASTM C773-88 (2011), using a special piece of equipment called Instron Model 3767. The rate used for these means was 1.3 mm/sec.

From the test data, variables corresponding to the extension, load and time elapsed until the full deformation of the foam were obtained for approximately 7000 ceramic foams. The extension referred to the mm deformed of the ceramic foam over time after a load was applied. The load data indicates the effort made by the team to compress the ceramic foam.

From the data obtained, a relationship between the load and the extent obtained was established (Figure 6), corresponding to the relationship between the extension and the load to the ceramic foam EC1, EC-2 and EC-3. Figure 7 shows that for mixtures of ceramic foams, the generated behaviour is similar mechanical resistance, and resistance capability changes. A decrease in resistance was seen with increasing content of feldspar and decreasing quartz content, which is consistent with the observation that it is the quartz which confers resistance to the ceramic foam and is responsible for the generation of pores during the sintering process.

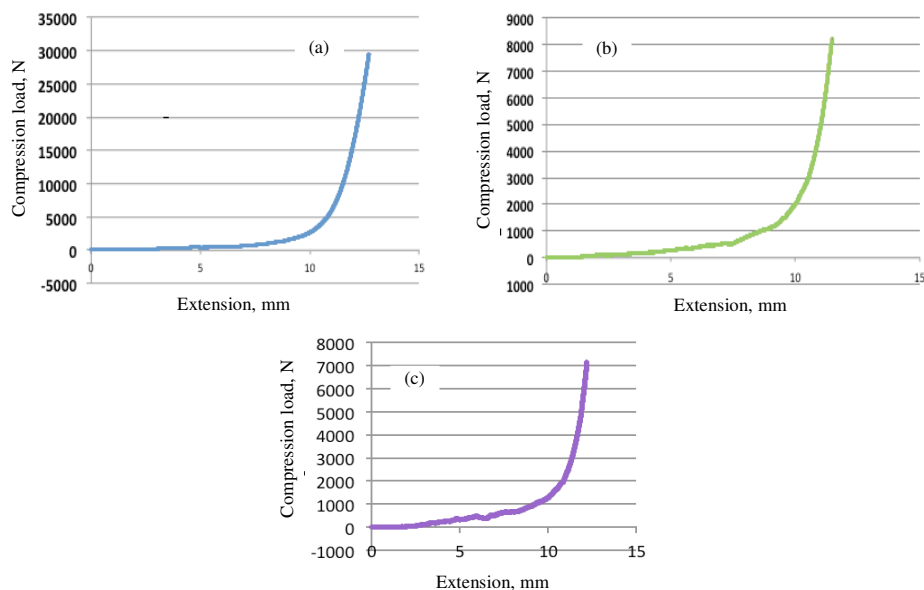


**Figure 6.** Intron test for ceramic foams: (a) Load vs. Extension EC-1, (b) Load vs. Extension EC-2 and (c) Load vs. Extension EC-3

According to the results shown in Figure 6, the ceramic foam EC-1 is the one with the greater resistance after applying the voltage for 10 minutes; the results allow us to establish that this is the foam that has the greater mechanical strength and for pilot-scale applications, has a higher probability of success.

#### *Analysis results for isotherms from aqueous solution $Cr^{3+}$ and $Ni^{2+}$ on the ceramic foams synthesised*

The adsorption isotherms for the three aqueous foams synthesised in this work are determined. To adjust the experimental results, a suitable model was used, adjusting the Langmuir and Freundlich models. The isotherms for the adsorption of  $Ni^{2+}$  from aqueous solution at controlled pH (pH = 5.0, in this work) on the ceramic foams are shown in Figure 7; adjustment to the Freundlich and Langmuir model was carried out as mentioned with activated carbons. In this study, no trends were plotted, which is presented in detail in Table 3. Correlation coefficients and constants corresponding to such models, for the adsorption of  $Cr^{3+}$  and  $Ni^{2+}$  on the foams were calculated.

**Table 3.** Correlation constants and coefficients of the models Langmuir and Freundlich of the isotherms for adsorption of  $Cr^{3+}$  and  $Ni^{2+}$  on the foams synthesised

	Langmuir			Freundlich		
	$q_e$ , mg/g	K, L/mg	$R^2$	$K_F$ , L/g	n	$R^2$
EC-1(Cr)	12.2134	0.01435	0.9732	12.6543	0.6549	0.9992
EC-2(Cr)	10.5763	0.01123	0.9632	7.9373	0.5469	0.9992
EC-3(Cr)	9.2145	0.01043	0.9765	4.9721	0.8734	0.9999
EC-1(Ni)	15.5433	0.02451	0.9387	10.4621	0.8765	0.9993
EC-2(Ni)	13.6598	0.02154	0.9675	8.4565	0.6573	0.9993
EC-3(Ni)	11.0543	0.01763	0.9833	6.8752	0.8735	0.9991



The results presented in Table 3 show that the regression coefficient ( $R^2$ ) of all materials are synthesised between 0.99993 and 0.99912 for Freundlich adsorption, suggesting that both  $\text{Ni}^{2+}$  and  $\text{Cr}^{3+}$  on foams can be described well by this model. Additionally, the values of  $n$  are between 0 and 1, which corroborates the previous statement, as this parameter with these values indicates that the interaction is favourable.

In Figures 7a and 7b, the maximum amount of  $\text{Ni}^{2+}$  and  $\text{Cr}^{3+}$  adsorbed respectively ( $q_e$ ) on different samples foams suggests that the sample EC-1 is the one that has the largest adsorptivity towards both ions under study. Here, we must emphasise that although that amount retained is not high compared with results using other materials reported in the literature, these results are very promising and novel in the development in the area of special materials, to continue in this direction and develop materials based foams on such structures since in the does not literature there are reports of this type, specially studies of adsorption of ions with ceramic foams in these experimental conditions. Table 3 shows that, based on the correlation coefficient, the best fit for the isotherms studied for the removal by adsorption of  $\text{Cr}^{3+}$  and  $\text{Ni}^{2+}$  at pH studied, is the Freundlich model.  $R^2$  values are close to unity, as mentioned in the previous paragraph, which enables this deduction, suggesting that the adsorption may be multilayer adsorption<sup>13-18</sup>.

These results suggest that foams have extensive porosity and a structure that allows fast diffusion of the pores within the structure until reaching its maximum adsorption capacity and that similar diameters generate an ionic adsorption capacity, as shown in Figure 7.

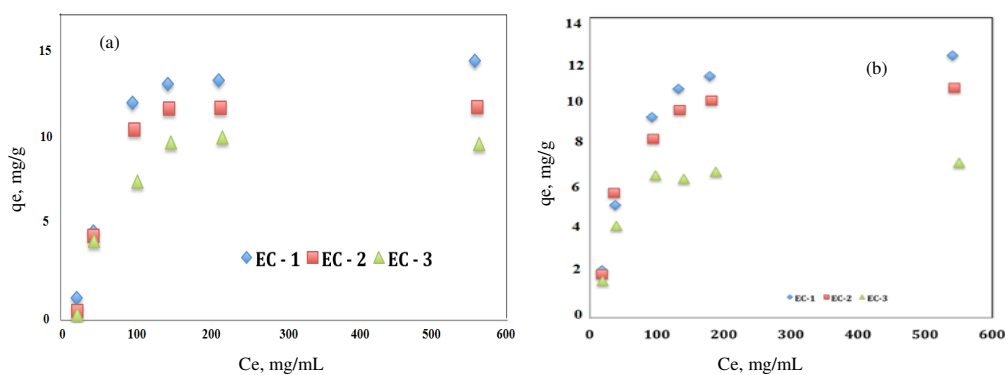


**Figure 7.** Isotherms of adsorption from aqueous solution on ceramic foams: (a)  $\text{Cr}^{3+}$  and (b)  $\text{Ni}^{2+}$

### *Conclusions of the adsorption of nickel and chromium on the ceramic foams*

The tests used in this research shows that materials were incorporated well in the synthesised foams. The results show that the composition in the preparation of ceramic foams directly influences the textural properties. The foam EC-1 had the greatest BET area of  $35 \text{ m}^2/\text{g}$ ; this suggested that the foam had the highest adsorption capacity for both ions, particularly of an amount of adsorbed  $\text{Cr}^{3+}$ , which was slightly higher compared to the  $\text{Ni}^{2+}$ ; this is due to the distribution of the porous ceramic foams and the difference in ionic size of these ions. The adsorption of ions was adjusted by the Freundlich model.

The present foam EC-1 was analysed by the increased resistance Instron test, which allows us to establish that this can be used more successfully to pilot plant level depositions ions in the aqueous phase.

### Acknowledgement

The authors thank the Master Agreement established between the University of the Andes and the University National of Colombia and the Memorandum of understanding established by the Departments of Chemistry from both the Universities. The authors express their thanks to Fondo de Investigaciones para estudiantes de Posgrado, de la Facultad de Ciencias de la Universidad de los Andes (Colombia) por su apoyo for the financial support

### References

1. Yajima S, Hayashi J and Omori M, *Chem Lett.*, 1975, **4(9)**, 931-934.
2. Scheffler M and Colombo P, *Cellular Ceramics: Structure, Manufacturing, Properties and Application*, Wiley-VCH, Weinheim, 2005, 645.
3. Hench L L and Polak J M, *Science*, 2002, **295(5557)**, 1014-1017.
4. Nonnenmacher K, Kleebe H J, Rohrer J, Ionescu E and Riede R, *J Am Chem Soc.*, 2013, **96(7)**, 2058-2056.
5. Gonzenbach U T, Studart A R, Tervoort E and Gauckler L J, *J Am Ceram Soc.*, 2007, **90(1)**, 16-22.
6. Rodriguez-Reinoso F, *Production and Applications of Activated Carbons In: Handbook of Porous Solids*. Eds., Schüth F, Sing K S W and Weitkamp J, Wiley-VCH, 2002.
7. Marsh H, Heintz E A and Rodriguez-Reinoso F, Eds., *Introduction to Carbon Technologies*. Universidad de Alicante, Spain, Secretariado de Publicaciones 1997.
8. Stoekli H F, *Carbon*, 1990, **28**, 1-12.
9. Reyes S A M, *Microscopía Electrónica y Microanálisis a la Solución de Problemas Geoquímicos*, VII Congreso Nacional de Geoquímica, Instituto de Geología, UNAM. 1997.
10. Guangqun T, Hongyan Y, Yong L and Dan X, *J Haz Mater.*, 2010, **174(1-3)**, 740-745.
11. Parab H, Joshi S, Shenoy N, Lali A, Sarma U S and Sudersanan M, *Proc Biochem.*, 2006, **41(3)**, 609-615.
12. Li Y S, Liu C C and Chiou C S, *J Colloid Interf Sci.*, 2004, **273(1)**, 95-101.
13. Rai D, Sass B M and Moore D A, *Inorg Chem.*, 1987, **26**, 345-349.
14. Bernhard M, Brinckman E E and Sadler P J, *The Importance of Chemical Speciation in Environmental Processes*, Springer, New York, USA, 1986.
15. Ibraheem O Ali, Mohamed S Thabet, Karam S El-Nasser, Ali M Hassan and Tarek M Salama, *Micro Mesop Mater.*, 2012, **160(15)**, 97-105.
16. Hameed B H and Rahman A A, *J Hazard Mater.*, 2008, **160**, 576-581.
17. Zhang J, Shi Q, Zhang C, Xu J, Zhai B and Zhang B, *Bioresour Technol.*, 2008, **99(18)**, 8974-8980.
18. Hameed B H, Chin L H and Rengaraj S, *Desalination*, 2008, **225(1-3)**, 185-198.